

Performance-Based Seismic Design: Avant-garde and code-compatible approaches

Dimitrios Vamvatsikos¹, Athanasia K. Kazantzi² and Mark A. Aschheim³

Abstract: Current force-based codes for the seismic design of structures use design spectra and system-specific behavior factors to satisfy one or two pre-defined structural limit-states. In contrast, performance-based seismic design aims to design a structure to fulfill any number of target performance objectives, defined as user-prescribed levels of structural response, loss, or casualties to be exceeded at a mean annual frequency less than a given maximum. First, a review of recent advances in probabilistic performance assessment is offered. Second, we discuss the salient characteristics of methodologies that have been proposed to solve the inverse problem of design. Finally, an alternative approach is proposed that relies on a new format for visualizing seismic performance, termed Yield Frequency Spectra (YFS). YFS offer a unique view of the entire solution space for structural performance of a surrogate single-degree-of-freedom oscillator, incorporating uncertainty and propagating it to the output response to enable rapid determination of a good preliminary design that satisfies any number of performance objectives.

CE Database subject headings: Seismic response; Earthquakes; Performance evaluation; Safety; Structural reliability

¹ Lecturer, School of Civil Engineering, National Technical Univ. of Athens, Greece (corresponding author). E-mail: divamva@mail.ntua.gr

² Research Engineer, J.B. ATE, Herakleion Crete, Greece. E-mail: kazantzi@mail.ntua.gr

³ Professor, Dept. of Civil Engineering, Santa Clara Univ., 500 El Camino Real
Santa Clara, CA 95053. E-mail: maschheim@scu.edu

19 **Author Keywords:** Performance-based design; Probabilistic methods; Uncertainty

20 **Introduction**

21 Earthquake engineering is a fascinating scientific field where multiple disciplines come
22 together to mitigate the threat of one of the deadliest natural hazards on Earth. Of immediate
23 concern is the entirety of the built environment that houses the majority of human societal
24 and economic activities. Earthquakes thus threaten immeasurable wealth, representing past
25 investments in existing infrastructure and ever-increasing future ones as new structures are
26 added or renovated yearly. Damage to the built infrastructure ricochets through the
27 transportation, communication, financial, cultural, and economic dimensions of society.
28 Recent seismic events, e.g., Northridge (1994), Kobe (1995), China (2008), Tohoku (2011),
29 have shown that despite considerable advances in research, we still have a long way to go:
30 while modern buildings have lower fatality rates, the staggering monetary losses and
31 disruption of function from seismic events can cripple entire cities, or even countries.

32 At the core of earthquake engineering stand the dual problems of assessment and design.
33 Assessment is the direct process of estimating structural behavior given the structure and the
34 hazard. Design is the inverse problem, whereby a structure, its members and properties are
35 established to achieve an acceptable behavior under the given seismic hazard. As typically
36 befits such dualities, the direct path of assessment is by far the simpler of the two. Thus,
37 while the earthquake engineering field has benefited enormously from recent advances in
38 computer science and technology, these have been realized in an asymmetric way. Important
39 solutions have mostly been achieved for the assessment problem—e.g., Fajfar and Dolsek
40 (2010) introduced the concept of performance quantification within a probabilistic context as
41 a viable approach for design. Therein, a structure's properties may be taken into account
42 together with the seismic hazard obtained by probabilistic seismic hazard analysis (PSHA) to

43 provide relatively accurate estimates of the distributions of structural demand, repair cost,
44 time-to-repair or even human casualties. While most of these capabilities are still only
45 available at the academic level, some of the benefits are influencing the new generation of
46 seismic codes dealing with the assessment of existing structures, such as EN1998-3 (CEN
47 2005) and ASCE/SEI 41-06 (2007), and in the establishment of design parameters for seismic
48 force-resisting systems, e.g., FEMA P-695 (2009) and FEMA P-795 (2011).

49 In contrast, no such revolution has been realized for routine design. Current seismic
50 design codes follow a classical force-based design paradigm that has been in place for
51 decades, in which design lateral forces are based on elastic demands reduced by a system-
52 specific “behavior” R - or q -factor to account for inelasticity. Generally, the smoothed
53 (pseudo-acceleration) design spectra and R - or q -factors are intended to approximately
54 achieve Life Safety performance for ground motions having a probability of exceedance of
55 about 10% in 50 years. The R - or q -factors are prescribed by the code, are specific to each
56 lateral load-resisting system type, and purportedly account for the ductility capacity and
57 overstrength inherent in buildings of various configurations, in view of local construction
58 practice. Demands at critical sections are determined by elastic analysis (static or dynamic) in
59 a simplified process that is intuitive to engineers. The design is deemed to provide acceptable
60 Life Safety performance simply by ensuring critical member sections have sufficient strength
61 and conform with prescribed detailing requirements. Serviceability is also addressed, by
62 limiting interstory drifts, either under the design lateral loads or for a reduced design
63 spectrum that relates to a more frequent level of seismic loads.

64 While the simplicity and utility of the classical approach is appealing, many drawbacks
65 exist. The emphasis on forces obscures the importance of stiffness, deformation demands,
66 mechanism development, and deformation compatibility. Moehle (1992) noted the value of
67 explicitly considering displacements in design, while Priestley (2000) promoted the use of an

68 equivalent linear approach to displacement-based design. Performance-based design
69 approaches often aim to limit drift and ductility demands and rely on displacement-based
70 approaches for doing so. Displacement-based approaches may be based on an estimate of the
71 fundamental period or the yield displacement of the structure in a first-mode pushover
72 analysis. The benefits of both force- and displacement-based approaches can be realized in
73 hybrid approaches that combine the two, as described recently by Tzimas et al. (2013).

74 Besides the emphasis on forces, another drawback of the classical approach is that
75 nonlinear effects are addressed only through the necessarily imprecise reduction/behavior
76 factor, while uncertainties are incorporated via safety factors at the input level of material and
77 load values instead of the output response. Under the severe demands of strong ground
78 shaking, this formulation leads to substantial variability in performance, which either leaves
79 some fraction of the building inventory vulnerable to deficient performance or wastes
80 resources in needlessly improving the performance of others, attempting to uniformly raise
81 the bar across a non-uniform population. A shift in paradigm is needed, from the present
82 emphasis on imbuing conservatism in the design of members to meet code requirements to
83 explicit accounting for uncertainty to achieve desired performance objectives for the specific
84 system.

85 Theoretical and practical difficulties have hampered the much sought-after leap to
86 performance-based seismic design, whereby a structure would be *directly designed* to satisfy
87 a range of performance objectives with specific allowable exceedance rates and explicit
88 consideration of uncertainty. The present paper responds to this challenge, providing a direct
89 way to incorporate uncertainty into a simple seismic design process that respects user-
90 determined limits on drift and system ductility. To lay the proper groundwork, the following
91 discusses the state-of-art in performance-based design, focusing on uncertainties, the
92 probabilistic basis of performance assessment, and salient characteristics of both

93 conventional and novel approaches to seismic design. In the end, the representation of
94 seismic demands using Yield Frequency Spectra (YFS) is offered as a new approach to
95 achieving performance targets with reasonable computational complexity.

96 **Current state of art**

97 ***Aleatory and epistemic uncertainty***

98 During the last decades, the use of probabilistic tools for assessing the reliability of structural
99 systems under seismic excitations has attracted considerable research worldwide (e.g.
100 Bazzurro et al. 1998, Cornell et al. 2002; Wen et al. 2003; Krawinkler and Miranda 2004).
101 Both assessment and design become more challenging when coupled within a probabilistic
102 framework, needed to account for the various sources of uncertainty sources that are intrinsic
103 to engineering applications. Uncertainties can be due to the inherently random nature
104 (aleatory), e.g., of seismic loads, or can be attributed to our incomplete knowledge
105 (epistemic), for example regarding the modeling or the actual properties of an existing
106 structure. The fundamental difference is that epistemic uncertainty can be reduced, for
107 example by conducting additional measurements, tests or experiments. However, aleatory
108 randomness is naturally occurring in a process, e.g., the sequence and magnitude of
109 earthquakes, and cannot be alleviated (at least not with any current or foreseeable
110 technology). In general, most existing performance-based assessment formats treat these two
111 flavors in a unified way (despite some objections, e.g., Der Kiureghian 2005) prompting us to
112 refer to them collectively as simply “uncertainty”.

113 So far, several researchers have concluded that, among all uncertainties, the ground
114 motion waveform has the most profound influence on the structural reliability, especially in
115 the case of performance levels associated with severe structural and non-structural damage
116 (Dymiotis et al. 1999; Kwon and Elnashai 2006; Kazantzi et al. 2008; Kazantzi et al. 2011).

117 A comprehensive site hazard representation that is compatible with current design norms is
118 provided by the seismic hazard surface, a 3D plot of the mean annual frequency (MAF) of
119 exceeding any level of spectral acceleration $S_a(T)$ for the full practical range of periods T
120 (Fig. 1). This is the true representation of seismic demands for elastic single-degree-of-
121 freedom (SDOF) oscillators at any given site. More familiar 2D pictures can be produced by
122 taking cross sections (or contours) of the hazard surface. Cutting horizontally at given values
123 of MAF will provide the corresponding uniform hazard spectra (UHS). For example, at
124 $P_o = -\ln(1 - 0.1)/50 = 0.0021$, or a 10% in 50 yrs probability of exceedance (Fig. 2a), one
125 obtains the spectrum typically associated with design at the ultimate limit state (or Life
126 Safety). Taking a cross section at a given period T produces the corresponding $S_a(T)$ hazard
127 curve (Fig. 2b).

128 Considerable uncertainty also may be introduced due to material properties and due to
129 the choice of model and analysis type. Details of soil, foundation and structural modeling
130 may heavily influence the outcome of any analysis method, as shown in Fig. 3 for the
131 capacity curve of a simple 5-story structure. With models under cyclic loading still under
132 development (e.g. Lignos and Krawinkler 2011) and with considerable uncertainty about
133 behavior in the high-deformation region (Fig. 4a), the accurate evaluation of structural
134 response within an analytical context remains a difficult task, and one that may lead to
135 inaccurate response estimates and consequently to structural designs with unsatisfactory or
136 non-homogeneous seismic reliability. This is particularly true in cases where simplified
137 modeling assumptions and analysis options have been employed and the structure approaches
138 its collapse capacity, where large deformations and complicated degradation come into play
139 as prominently shown in Fig. 4b (see also Villaverde 2007).

140 **Performance-based assessment**

141 Performance-based earthquake engineering has recently emerged to quantify in probabilistic
142 terms the performance of structures using metrics that are of immediate use to both engineers
143 and stakeholders (Yang et al. 2009). The use of a proper probabilistic framework for
144 propagating both aleatory and epistemic uncertainties to the final results obtained from a
145 variety of nonlinear analysis methods (e.g. static pushover and nonlinear response history
146 analysis) is best exemplified by the Cornell-Krawinkler framing equation adopted by the
147 Pacific Earthquake Engineering Research (PEER) Center (Cornell and Krawinkler 2000):

148
$$\lambda(DV) = \iiint G(DV | DM) |dG(DM | EDP)| |dG(EDP | IM)| |d\lambda(IM)| \quad (1)$$

149 for which DV is one or more decision variables, such as cost, time-to-repair or human
150 casualties that are meant to enable decision-making by the stakeholders; DM represents the
151 damage measures, typically discretized in a number of progressive damage states for
152 structural and non-structural elements and even building contents; EDP contains the
153 engineering demand parameters such as interstory drift or peak floor acceleration that the
154 engineers are accustomed to using when determining the structural behavior; and, IM is the
155 seismic intensity measure, for example represented by the 5%-damped first-mode spectral
156 acceleration $S_a(T_1)$. The relationship of EDP and IM is obtained by structural analysis and can
157 be established through incremental dynamic analysis (IDA, Vamvatsikos and Cornell 2002),
158 using multiple ground motion records scaled to different intensity levels (and exceedance
159 frequencies). An example is shown in Fig. 5, where even for an SDOF system, considerable
160 variability is present. The function $\lambda(y)$ provides the MAF of exceedance of values of its
161 operand y , thus making $\lambda(IM)$ the seismic hazard, while $G(x)$ is the complementary
162 cumulative distribution function (CCDF) of its variable x . Finally, note that all differentials in
163 Eq. (1) appear as absolute values since they concern monotonically decreasing functions, and
164 thus they would otherwise be negative.

165 Stakeholders care about DV and perhaps even DM , or damage states. Engineers, on the
166 other hand, prefer to focus on EDP to express performance. This may be best achieved by
167 moving to the familiar territory of limit states and appropriately modifying the Cornell-
168 Krawinkler framing equation (Vamvatsikos and Cornell 2004). Defining DV and DM to be
169 simple indicator variables that become 1.0 when a given limit-state (LS) is exceeded,
170 transforms Eq. (1) to estimate λ_{LS} , the MAF of violating LS:

$$171 \quad \lambda_{LS} = \int G(EDP | IM) |d\lambda(IM)| \quad (2)$$

172 Both approaches represented by Eq. (1) and Eq. (2) find excellent uses but they are
173 presently limited to assessment, i.e., the forward derivation of a given structure's
174 performance. A proper performance-based design would mean at least inverting such
175 equations to allow deriving the desired properties of the structure that would satisfy a given
176 value of λ_{LS} , for example the 0.002 per annum to successfully fulfill the Life Safety
177 requirements. Closed-form approximations of the integral in Eq. (2) can offer significant help
178 in achieving such a design-oriented solution. The best known such expression is offered by
179 Cornell et al. (2002), using a power-law approximation for both the hazard curve and the
180 median EDP versus IM relationship. To improve the inherent accuracy issues (see Bradley
181 and Dhakal 2008), Lazar and Dolsek (2014) have suggested the introduction of appropriate
182 integration bounds, while Vamvatsikos (2014) has recommended the use of a biased fit to the
183 hazard curve that favors lower intensities, and/or the introduction of a second-order power-
184 law approximation for the hazard curve.

185 ***Design approach characteristics***

186 Each approach to design has its own characteristics in terms of how the design problem is
187 defined and how one goes about solving it. The design problem is essentially an optimization
188 problem, where specific performance objectives are set and an approach is offered on how to

189 achieve them. How these objectives are defined and what approach is taken to meet them is
190 what essentially establishes the basis of design. In the following we distinguish different
191 methodologies that have appeared in the literature based on three essential characteristics:
192 how one chooses to (a) express the performance targets, (b) treat uncertainty, and (c) connect
193 performance targets to the design of members and thus solve the optimization problem.

194 **Performance targets**

195 Each performance objective can be thought of as a specific value of a “performance variable”
196 paired with a (maximum allowable) target MAF of exceeding it. Eqs (1) and (2) represent
197 two different approaches for defining the performance variable and estimating the
198 corresponding MAF. For example, let us consider a Life Safety performance objective tied to
199 the well-known 10% probability of exceedance in 50 years, or MAF of 0.0021. The
200 difference in employing Eq. (1) versus Eq. (2) appears in the metrics used to define Life
201 Safety itself. In Eq. (1) this is expressed in terms of one or more DVs, for example by
202 requesting casualties less than $x\%$ of the inhabitants and property damage less than $y\%$ of the
203 total investment at the given MAF. In Eq. (2), this could be a more familiar limitation in
204 terms of one or more EDPs, e.g., having a maximum interstory drift ratio lower than 2% at
205 the given MAF without any brittle failure of structural components.

206 While being able to design a structure that can satisfy performance objectives that
207 actually make sense to stakeholders may be considered to be the ultimate goal of
208 performance-based design, estimating such losses is not a trivial procedure (see Baker and
209 Cornell 2008). Absent crude approximations for seismic losses, only full-scale optimization
210 approaches can accurately solve this problem. A prime example of the challenges involved in
211 properly accounting for seismic losses in design is offered by the conceptual approach of
212 Krawinkler et al. (2006).

213 **Propagation of uncertainty**

214 The uncertainty in seismic hazard is of such magnitude that a design method that does not
215 account for it is inconceivable. The difference among design methods is in the way that this
216 uncertainty is taken into account. Herein, performance objectives were explicitly defined as
217 specific DV or EDP values tied to a target MAF, the latter conveying the probabilistic nature
218 of the (output) measure of performance of the design. In contrast, the typical approach is to
219 consider hazard uncertainty at the input intensity level, i.e., by designating the MAF of
220 exceeding specific IM levels of the (input) ground motion. This is incorporated in all current
221 design codes, in the form of the (smoothed) uniform hazard design spectra (see Fig. 2a) that
222 contain all the $S_a(T_1)$ values that correspond to a given MAF of exceedance. By subjecting the
223 structure to forces consistent with such a spectrum one derives the output values of DV or
224 EDP; if the limit is not violated, the design complies with code requirements and is deemed
225 adequate (although the MAF of exceedance of the DV or EDP remains unknown).

226 Code design formats have their roots in the partial safety factor approach (load and
227 resistance factor design) that is generally used in the linear (or near-linear) range of structural
228 response. Therein, the linear equations that tie the loads and their effects essentially ensure
229 that uncertainty applied at the input is properly propagated to the output, at least in terms of
230 preserving the first and second moment (mean and variability), if not the distribution type. On
231 the other hand, the nonlinearity that is inherent in extreme seismic events means that no such
232 assumptions can be made. Further to this point, Cornell et al. (2002) showed that the shape of
233 the hazard curve and the variability in the EDP–IM relationship mean that multiple hazard
234 levels need to be considered to evaluate performance. Actually, since the lognormal
235 distribution of EDP given IM has a heavy right tail (i.e., a high proportion of extreme
236 responses) and the lower IM values appear more frequently (i.e., correspond to a higher MAF
237 of exceedance in Fig. 2b), they contribute significantly more to the system's rate of exceeding

238 any limit-state. For example, the MAF of exceedance of a prescribed (output) EDP value is
239 guaranteed to be higher than the MAF of the (input) IM that it corresponds to, on average,
240 often by factors higher than 100%. Thus, whenever probability is controlled/applied/checked
241 at the input intensity of a nonlinear structure, it will often result to a (mean) output of
242 unknown magnitude.

243 The inconsistency of specifying probability at the input rather than the output
244 undermines the probabilistic basis of all such approaches and becomes an important liability.
245 There is truly no “right” value for the safety factors (typically incorporated within material
246 safety factors and the conservativeness in choosing R , q) that can be both *safe* and
247 *economical* when applied to an entire class of buildings. Designs complying with code
248 requirements may be too safe (and therefore, costly) or the opposite, as blanket safety factors
249 do not provide the same performance across the range of building configurations (or
250 archetypes, in the terminology of FEMA P-695 (2009)) allowed within a building code. As
251 well, since the calibration of code design parameters results in a range of performance for
252 code compliant designs, it is not clear what (stricter) performance criteria should be imposed
253 to obtain user-prescribed “better than code” performance. The use of importance factors to
254 amplify the design spectrum or equivalently, reduce demands for the given design spectrum,
255 are an imprecise substitute. Only design formats that accurately propagate the uncertainty
256 from input IM to output DV or EDP and are theoretically consistent can allow the MAF of
257 exceedance of the output to be controlled; this is necessary in our opinion for a design
258 approach to truly be “performance-based”.

259 **Design solution process**

260 Having defined the performance objectives, the grand question of how one goes about
261 establishing a structure that can meet them must be addressed. All design approaches are
262 essentially methods to solve this inverse problem, which is challenging because the

263 functional relationship between the design variables, e.g., member sizes, and the target
264 objectives is not invertible, and may not be precisely known. Thus, iteration is required.
265 Engineers can easily solve the forward problem of applying the “seismic loads” to determine
266 individual member forces or deformations and invert (explicitly or implicitly through
267 iterations) the equations that define section or member resistance to derive the minimum
268 required member size. The question is how to determine the loads to apply, since (a) they
269 depend on the dynamic characteristics of the yet to be determined structure and (b) they need
270 to be consistent with the design objectives. Here one needs to choose between working with
271 the multi-degree-of-freedom (MDOF) system using a simpler proxy, or making use of a
272 database (or sequence) of relevant candidate MDOF designs.

273 Assessing the performance of candidate MDOF designs is a conceptually simple direct-
274 search problem that is well suited to optimization. At its simplest implementation, an
275 engineer is guided by his/her intuition to incrementally change an initial design to
276 satisfaction. Each iteration, though, is equivalent to a cycle of re-design and re-analysis,
277 where the latter is a full-blown performance-based assessment involving nonlinear static or
278 dynamic runs, as discussed in Krawinkler et al. (2006). Any method built on this paradigm
279 essentially is an iterated assessment procedure. Many researchers have also chosen to
280 improve upon the efficiency of the re-design to achieve a fast convergence, often leading to
281 the use of numerical optimization. An optimization algorithm provides candidate structures
282 for performance assessment. Force and deformation checks are encoded as constraints, while
283 the initial or lifecycle cost of the structure can be the optimization objective (Fragiadakis and
284 Lagaros 2011). Mackie and Stojadinovic (2007) have suggested this approach for bridges
285 while Fragiadakis and Papadrakakis (2008), Franchin and Pinto (2012) and Lazar and Dolsek
286 (2012) have all used optimization techniques for the performance-based seismic design of
287 reinforced-concrete structures.

288 While using the MDOF system is arguably more comprehensive and accurate, it is also
289 considerably more expensive. A simpler approach entails using a surrogate system, typically
290 an SDOF oscillator, to help translate the MAFs of exceedance of EDP limits to design loads.
291 Thus, the complexity of guessing the MDOF system's properties is reduced to determining
292 the strength and stiffness that define the surrogate oscillator (often assumed to have elasto-
293 plastic behavior). Any two of the following quantities define the oscillator yield point: (a)
294 period, T , (b) yield strength, F_y , (usually normalized by the (known) weight W to equal the
295 base shear coefficient at yield, $C_y = F_y / W$), and (c) yield displacement, δ_y . These three
296 quantities are functionally related:

$$297 \quad T = 2\pi \sqrt{\frac{\delta_y}{C_y g}} \quad (3)$$

298 Assuming now that a structural configuration has been decided, one needs only to
299 determine the minimal member sizes that satisfy the objectives. This is essentially akin to a
300 Newton-Raphson algorithm for finding the root (or minimum) of a nonlinear “black-box”
301 equation: a local estimate of the function tangent is employed and assumed to remain
302 constant to linearize the problem in order to point to a potential solution. This tangent is
303 essentially an assumed invariant term that is updated at the end of each iteration until
304 convergence. Presently, there are two distinct flavors of the SDOF-proxy approach, based on
305 what term is considered to be *invariant* (or approximately stable).

306 Force-based approaches are the basis of practically all current seismic codes, and operate
307 on an invariant T basis. This is in turn used to determine $S_a(T)$ that is multiplied by the system
308 mass m (hence the “force-basis”) and divided by the ubiquitous R or q factor to determine the
309 desired base shear at yield, V_y . For a given mass, the same information as V_y is conveyed by
310 the spectral acceleration at yield, $S_{ay}(T)$, or similarly, C_y where $C_y = S_{ay}$ when S_{ay} is expressed
311 in units of g . The R - or q -factors are approximate methods to account for the effect of

312 overstrength and ductility on peak response. Note that while higher mode periods can be used
313 to determine the loads in a modal response analysis, the approach remains essentially SDOF-
314 based as R and q always refer back to the first mode only. The MDOF structure is then
315 designed to be safe against the required effects of loads consistent with C_y . An eigenvalue
316 analysis of the newly designed system provides an updated period and if a significant
317 difference is found, a new cycle of design and analysis is performed. A key feature of this
318 approach is the use of approximate formulas to provide an initial guess for T . A good guess
319 essentially eliminates the need for repeated cycles, something that is often the case when an
320 experienced engineer is facing a structure and associated performance objectives he/she is
321 comfortable with. Nevertheless, inaccurate estimates may be expected where more stringent
322 performance objectives call for more than usual lateral stiffness.

323 Alternatively, one may assume instead that the yield displacement δ_y is the invariant
324 term. This has been suggested by Priestley (2000) and Aschheim (2002) as a much more
325 stable parameter compared to the period T , thus significantly reducing the need for iterations.
326 Here, the design process starts by deriving an initial guess for δ_y (rather than T), and then
327 using derived limits on ductility, μ , and appropriate R - μ - T relationships to determine the
328 seismic coefficient C_y . The process has been encoded by Aschheim (2002) into a visual
329 design tool termed Yield Point Spectra (Fig. 6). Having established C_y , member sizes may be
330 determined. In the infrequent cases where iteration on δ_y is needed, a new yield displacement
331 is derived and the process is repeated. The refinement of the yield displacement is much like
332 the refinement of period that occurs in current force-based methods of design.

333 Table 1 summarizes the defining characteristics of different design approaches.
334 Practically all code-sanctioned methods use an EDP-basis and a force-based SDOF proxy,
335 while lacking uncertainty propagation. This description covers nearly 100% of current
336 engineering practice. At the academic level, considerable advances have appeared in the

337 MDOF-based indirect approach for performance-based design, often employing proper
338 uncertainty propagation and either an EDP (Franchin and Pinto 2012) or a DV basis (Mackie
339 and Stojadinovic 2007). Still, there are considerable usability barriers in adopting such
340 powerful approaches in practice. A methodology that, in the terms of Table 1, employs full
341 uncertainty propagation, an EDP-basis and a displacement-invariant SDOF proxy to achieve
342 “directness” may have a better chance. Only recently, Vamvatsikos and Aschheim (2015)
343 proposed such a methodology to correctly propagate uncertainty at the SDOF level through
344 the use of YFS.

345 **Origin, definition, and use of Yield Frequency Spectra**

346 The essential ingredients of the YFS approach to performance-based design are (a) the site
347 hazard and (b) some assumption about the system’s behavior (e.g. elastic, elastoplastic, etc)
348 that is used to define the SDOF proxy. Then, for a given capacity curve shape (or system
349 type) we are asked to estimate the yield strength and the period, T , for not exceeding a
350 limiting displacement δ_{lim} at a rate higher than P_o . Even for an SDOF system, the introduction
351 of yielding, ductility and the resulting record-to-record response variability fundamentally
352 changes the nature of the problem. This is best represented in the familiar coordinates of the
353 IM, taken here as the first mode spectral acceleration $S_a(T)$, and the EDP, i.e., the
354 displacement response δ . The structural response then appears in the form of IDA curves as
355 shown in Fig. 5 for a $T = 1$ s system with a capacity curve having positive and then negative
356 post-yield stiffness. Formally, this relationship may be represented by the following integral
357 (Jalayer 2003; Vamvatsikos and Cornell 2004), that is equivalent to Eq. (2):

$$358 \quad \lambda(\delta) = \int_0^{+\infty} P[EDP > \delta | IM = s] |d\lambda(s)| \quad (4)$$

359 where $P[EDP > \delta | IM = s]$ is the probability of exceeding a certain level of response δ
360 given a seismic intensity of s , equivalent to $G(EDP | IM)$, the CCDF of EDP given IM
361 evaluated at specific values of each (e.g., Fig. 5). $\lambda(s)$ is the associated hazard rate.

362 Using Eq. (4) together with R - μ - T relationships that offer the probabilistic distribution of
363 structural response given intensity $P[EDP > \delta | IM = s]$ (e.g. Vamvatsikos and Cornell
364 2006), rather than just the mean, allows the estimation of the so-called inelastic displacement
365 (or drift) hazard curves. For a yielding system these are the direct equivalent of spectral
366 displacement hazard curves. They have appeared at least in the work of Inoue and Cornell
367 (1990) and subsequently further discussed by Bazzurro and Cornell (1994) and Jalayer
368 (2003). While useful for assessment, they lack the necessary parameterization to become
369 helpful for design. An appropriate normalization may be achieved for oscillators with yield
370 strength and displacement F_y and δ_y , respectively, by employing ductility μ , rather than
371 displacement δ and the seismic coefficient C_y instead of the strength.

372 Up to this point, what has been proposed is similar to the results presented by Ruiz-
373 Garcia and Miranda (2007) on the derivation of maximum inelastic displacement hazard
374 curves. What truly makes the difference is defining δ_y as a constant for a given structural
375 system, for relevance to displacement-based design. Then C_y essentially replaces the period
376 T , as expressed in Eq. (3).

377 For a given site hazard and oscillator properties—system damping, δ_y , value of C_y (or
378 period), and capacity curve *shape* (e.g. as normalized in terms of $R = F/F_y$ and μ)—a unique
379 representation of the oscillator's probabilistic response may be gained through the
380 displacement (or ductility) hazard curves produced via Eq. (4). Damping, δ_y and the capacity
381 curve shape are considered as stable system characteristics, as they would be in a
382 displacement-based design process. By plotting such curves of $\lambda(\mu)$, for a range of μ_{lim}
383 limiting values and a range of C_y , we obtain contours of the inelastic displacement hazard

384 surface for constant values of C_y . These contours allow the direct evaluation of system
385 strength and period—i.e., the C_y required to satisfy any combination of performance
386 objectives defined as $P_o = \lambda(\mu_{lim})$, where each limiting value of ductility μ_{lim} is associated with
387 a maximum MAF of exceedance P_o , as shown in Fig. 7.

388 The resulting YFS are thus proposed as a design aid, being a direct visual representation
389 of a system's performance that quantitatively links the MAF of exceeding any displacement
390 value (or ductility μ) with the system yield strength (or seismic coefficient C_y). YFS are
391 plotted for a specified yield displacement; thus, periods of vibration represented in YFS vary
392 with C_y . Fig. 7 presents an example for an elastic-perfectly-plastic oscillator. In this case,
393 three performance objectives are specified (the red "x" symbols) while curves representing
394 the site hazard convolved with the system fragility are plotted for fixed values of C_y . Of
395 course, increases in C_y always reduce the MAF of exceeding a given ductility value. Thus,
396 the minimum acceptable C_y (within some tolerance) that fulfils the set of performance
397 objectives for the site hazard can be determined for an SDOF system. This strength is used as
398 a starting point for the performance-based design of more complex structures, potentially
399 solving the problem in a single step having begun with a good estimate of the yield
400 displacement.

401 At a certain level, YFS can be considered as a building- and user-specific extension of
402 concepts behind the IBC (2011) risk-targeted design spectra. Whereas the latter are meant to
403 offer a uniform measure of safety, they only do so for one limit-state (global collapse), one
404 specific target probability (1% in 50 years) and a given assumed fragility regardless of the
405 type of lateral-load resisting system. On the contrary, YFS can target any number of
406 concurrent limit-states, each for a user-defined level of performance (or safety), and employ
407 building-specific fragility functions, as implied by the supplied capacity curve shape. The
408 practical estimation of YFS is thus based on the case-by-case solution of the integral in

409 Eq. (4). This involves a comprehensive evaluation for a number of SDOF oscillators with the
410 same capacity curve shape and yield displacement but different periods and yield strengths. If
411 a numerical approach is employed, then we can obtain the comprehensive view shown in
412 Fig. 7 at the cost of a few minutes of computer time. Alternatively, if one seeks only the
413 value of C_y corresponding to each performance objective, then an analytical approach can be
414 used that offers accurate results with only a few iterations (Vamvatsikos and Aschheim
415 2015).

416 As an example of application, we consider an $H = 32.8\text{m}$ high, 8-story reinforced-
417 concrete space-frame building (from FEMA 2009) to be designed for a high-seismicity site
418 having a (10% in 50 year) design spectrum anchored at $S_a(0.5\text{s}) = 1.5\text{g}$ and falling off with
419 $1/T$ in the period range of interest. A yield displacement of 0.22m (0.67% yield roof drift)
420 was determined for the MDOF system, translated to 0.13m for the equivalent SDOF
421 (Vamvatsikos et al. 2015), while a serviceability requirement of 0.75% maximum interstory
422 drift was adopted at the 10% in 10 years frequency (or a MAF of 0.0105), becoming the
423 governing performance target. For a ratio of maximum interstory drift to roof drift of about
424 1.5, this translated to a ductility limit of $\mu = 0.75\% / (1.5 \cdot 0.67\%) = 0.76$. A simplified model
425 of the hazard was employed (Cornell et al. 2002), assuming hazard curves of constant slope k
426 $= 2.5$ in lognormal coordinates. As solution was sought in the *nominally* elastic region ($\mu < 1$)
427 a low, yet non-zero, dispersion of 20% was assumed for the response distribution in Eq. (4).
428 YFS suggested a required first-mode period (cracked section properties) of $T = 1.24\text{s}$ and a
429 yield base shear of $V_y \approx 2500\text{kN}$. Having determined member sizes for the entire structure on
430 these two premises, performance was assessed through IDA. The MAF of violating the
431 serviceability limit-state was found to be 0.0097, i.e., lower than the 0.0105 threshold,
432 soundly validating the proposed approach.

433 **Conclusions**

434 There are many published design approaches for achieving the desired performance
435 compliance for any structure. Current code approaches are arguably the simplest and most
436 practical ones. Yet, they are invariably limited in accuracy due to their far-from-perfect
437 handling of uncertainty, which can severely bias the output design to be either too
438 conservative, or even unconservative, and with unknown MAFs of exceedance. Furthermore,
439 their use of a force-basis means that some iterations may be needed, unless a good
440 approximation of the desired period is available. On the other end of the spectrum lie the
441 modern methods that employ full system optimization to achieve the required performance in
442 terms of reducing actual seismic losses. These may truly fulfill the actual target of
443 performance-based design, yet they are severely encumbered by their computational
444 complexity. Most, if not all, are only applicable within an academic environment. Attempting
445 to bridge this distance, Yield Frequency Spectra have been introduced as an intuitive and
446 practical approach to performance-based design. They allow design to approximately satisfy
447 an arbitrary number of performance objectives that can be connected to the global
448 displacement of an equivalent single-degree-of-freedom oscillator. Within this relatively
449 benign constraint, our approach incorporates uncertainty and accurately propagates it to the
450 output structural response, where performance is checked. Thus, it can help deliver
451 preliminary designs that are close to their performance targets, requiring few (if any) cycles
452 of re-analysis and re-design to reach the final stage. Only time will tell if engineering practice
453 is ready to adopt a new design paradigm.

454 **Acknowledgements**

455 Financial support was provided by the European Research Executive Agency via Marie Curie
456 grant PCIG09-GA-2011-293855 and by Greece and the European Social Funds through the

457 Operational Program “Human Resources Development” of the National Strategic Framework
458 (NSRF) 2007-2013.

459 **References**

460 Aschheim, M. (2002). “Seismic design based on the yield displacement.” *Earthq. Spectra*, 18(4),
461 581–600.

462 ASCE (2007). “Seismic Rehabilitation of Existing Buildings.” *ASCE/SEI 41-06*, American Society of
463 Civil Engineers, Structural Engineering Institute, Reston, VA.

464 Baker, J. W., and Cornell, C. A. (2008). “Uncertainty propagation in probabilistic seismic loss
465 estimation.” *Struct. Safety*, 30, 236–252.

466 Bazzurro, P., and Cornell, C. A. (1994). “Seismic hazard analysis of nonlinear structures. II:
467 Applications.” *J. Struct. Engng*, 120(11), 3345–3365.

468 Bazzurro, P., Cornell, C. A., Shome, N., and Carballo, J. E. (1998). “Three proposals for
469 characterizing MDOF nonlinear seismic response.” *J. Struct. Engng*, 124(11), 1281–1289.

470 Bradley, B. A., and Dhakal, R. P. (2008). “Error estimation of closed-form solution for annual rate of
471 structural collapse.” *Earthq. Eng. Struct. Dyn.*, 37(15), 1721–1737.

472 CEN (2005). “Eurocode 8: Design of structures for earthquake resistance — Part 3: Assessment and
473 retrofitting of buildings.” *EN1998-3*, European Committee for Standardization, Brussels.

474 Cornell, C.A., Jalayer, F., Hamburger, R.O., and Foutch, D.A. (2002). “The probabilistic basis for the
475 2000 SAC/FEMA steel moment frame guidelines.” *J. Struct. Engng*, 128(4), 526–533.

476 Cornell, C.A., and Krawinkler, H. (2000). “Progress and challenges in seismic performance
477 assessment.” *PEER Center News* 3 (2), 2000. URL
478 <http://peer.berkeley.edu/news/2000spring/index.html>, (Feb. 14, 2014).

479 Der Kiureghian, A. (2005). “Non-ergodicity and PEER’s framework formula.” *Earthq. Engng Struct.*
480 *Dyn.*, 34, 1643–1652.

481 Dymiotis, C., Kappos, A. J., and Chryssanthopoulos, M. K. (1999). "Seismic reliability of RC frames
482 with uncertain drift and member capacity." *J. Struct. Engng*, 125(9), 1038–1047.

483 Fajfar P., and Dolsek, M. (2010). "A practice-oriented approach for probabilistic seismic assessment
484 of building structures." *Advances in Performance-Based Earthquake Engineering, Geotechnical,
485 Geological, and Earthquake Engineering (Fardis M.N. ed.)*, Chapter 21, Springer, Dordrecht.
486 DOI 10.1007/978-90-481-8746-1_21.

487 FEMA (2009). "Quantification of Building Seismic Performance Factors." *Rep. No. FEMA P-695*,
488 prepared by Applied Technology Council for the Federal Emergency Management Agency,
489 Washington, D.C.

490 FEMA (2011). "Quantification of Building System Performance and Response Factors - Component
491 Equivalency Methodology." *Rep. No. FEMA P-795*, prepared by Applied Technology Council,
492 prepared for the Federal Emergency Management Agency, Washington, D.C.

493 Fragiadakis, M., and Lagaros, N. D. (2011). "An overview to structural seismic design optimisation
494 frameworks." *Comput. Struct.*, 89, 1155–1165.

495 Fragiadakis, M. and Papadrakakis, M. (2008). "Performance-based optimum seismic design of
496 reinforced concrete structures." *Earthq. Engng Struct. Dyn.*, 37, 825–844.

497 Franchin, P., and Pinto, P. (2012). "Method for probabilistic displacement-based design of RC
498 structures." *J. Struct. Engng*, 138 (5), 585–591.

499 IBC (2011). "2012 International Building Code." International Code Council, IL.

500 Inoue, T., and Cornell, C. A. (1990). "Seismic hazard analysis of multi-degree-of-freedom structures."
501 *Report RMS-08*, Reliability of Marine Structures Program, Stanford University, Stanford, CA,.

502 Jalayer, F. (2003). "Direct probabilistic seismic analysis: Implementing non-linear dynamic
503 assessments." *PhD Dissertation*, Department of Civil and Environmental Engineering, Stanford
504 University, Stanford, CA.

505 Kazantzi, A. K., Righiniotis, T. D., and Chryssanthopoulos, M. K. (2008). "Fragility and hazard
506 analysis of a welded steel moment resisting frame." *J. Earthq. Engng*, 12(4), 596–615.

507 Kazantzi, A. K., Righiniotis, T. D., and Chryssanthopoulos, M. K. (2011). "A simplified fragility
508 methodology for regular steel MRFs." *J. Earthq. Engng*, 15(3), 390–403.

509 Krawinkler, H., Zareian, F., Medina, R. A., and Ibarra, L.F. (2006). "Decision support for conceptual
510 performance-based design." *Earthq. Engng Struct. Dyn.*, 35(1), 115–133.

511 Krawinkler, H., and Miranda, E. (2004). "Performance-based earthquake engineering." *In: Bozorgnia,*
512 *Y., Bertero, V.V. (eds). Earthquake engineering: from engineering seismology to performance-*
513 *based engineering.* CRC Press, New York.

514 Kwon, O. S., and Elnashai, A. (2006). "The effect of material and ground motion uncertainty on the
515 seismic vulnerability curves of RC structure." *Engng Struct.*, 28(2), 289–303.

516 Lazar N., and Dolsek M., (2014). "Incorporating intensity bounds for assessing the seismic safety of
517 structures: Does it matter?" *Earthq. Engng Struct. Dyn.*, 43, 717–738

518 Lazar, N., and Dolsek, M. (2012). "Risk-based seismic design - An alternative to current standards for
519 earthquake-resistant design of buildings." *Proceedings of the 15th World Conference on*
520 *Earthquake Engineering*, Lisbon, Portugal.

521 Lignos, D. G., and Krawinkler, H. (2011). "Deterioration modeling of steel components in support of
522 collapse prediction of steel moment frames under earthquake loading". *J. Struct. Engng*, 137(11),
523 1291–1302.

524 Mackie, K. R., and Stojadinovic, B. (2007). "Performance-based seismic bridge design for damage
525 and loss limit states." *Earthq. Engng Struct. Dyn.*, 36, 1953–1971.

526 Moehle, J. P. (1992). "Displacement-Based Design of RC Structures Subjected to Earthquakes."
527 *Earthq. Spectra*, 8(3), 403–427.

528 Priestley, M. J. N. (2000). "Performance based seismic design." *Bull. New Zealand Society for*
529 *Earthq. Engng*, 33(3), 325–346.

530 Ruiz-Garcia, J., and Miranda, E. (2007). "Probabilistic estimation of maximum inelastic displacement
531 demands for performance-based design." *Earthq. Engng Struct. Dyn.*, 36:1235–1254.

532 Tzimas, A. S., Karavasilis, T. L., Bazeos, N., and Beskos, D. E. (2013). "A hybrid force/displacement
533 seismic design method for steel building frames." *Engng Struct.*, 56, 1452-1463.

534 Vamvatsikos, D. (2014). "Accurate application and second-order improvement of SAC/FEMA
535 probabilistic formats for seismic performance assessment." *J. Struct. Engng*, **140**(2), 04013058.

536 Vamvatsikos D., and Aschheim, M. A. (2015). "Performance-based seismic design via Yield
537 Frequency Spectra." *Earthq. Engng Struct. Dyn.*, (in review).

538 Vamvatsikos, D., and Cornell, C. A. (2002). "Incremental dynamic analysis." *Earthquake Eng. Struct.*
539 *Dyn.*, 31(3), 491–514.

540 Vamvatsikos, D. and Cornell, C. A. (2004). "Applied incremental dynamic analysis." *Earthq. Spectra*,
541 20(2), 523–553.

542 Vamvatsikos, D., and Cornell, C. A. (2006). "Direct estimation of the seismic demand and capacity of
543 oscillators with multi-linear static pushovers through Incremental Dynamic Analysis." *Earthquake Eng. Struct. Dyn.*, 35(9), 1097–1117.

544

545 Vamvatsikos, D., and Fragiadakis, M. (2010). "Incremental dynamic analysis for estimating seismic
546 performance uncertainty and sensitivity." *Earthquake Eng. Struct. Dyn.*, 39(2), 141–163.

547 Vamvatsikos D., Katsanos E. I., and Aschheim M. A. (2015). A case study in performance-based
548 design using yield frequency spectra. *Proc. SECED 2015 Conf.*, Cambridge, UK

549 Villaverde, R. (2007). "Methods to assess the seismic collapse capacity of building structures: state of
550 the art." *J. Struct. Engng*, 133(1), 57–66.

551 Wen, Y. K., Ellingwood, B. R. , Veneziano, D., and Bracci, J. (2003). "Uncertainty Modeling in
552 Earthquake Engineering." *MAE Center Project FD-2 Report*, Urbana, IL.

553 Yang, T. Y., Moehle, J., Stojadinovic, B., Der Kiureghian, A. (2009). "Seismic performance
554 evaluation of facilities: Methodology and implementation." *J. Struct. Engng*, 135(10), 1146–
555 1154.

556 Zeris, C., Vamvatsikos, D., Giannitsas, P., and Alexandropoulos, K. (2007). "Impact of FE modeling
557 in the seismic performance prediction of existing RC buildings." *Proc. COMPDYN2007 Conf.*
558 *on Comp. Methods in Struct. Dyn. and Earthq. Engng*, Rethymno, Greece.

559

560 **Figure Captions**

561 **Fig. 1.** Spectral acceleration hazard surface.

562 **Fig. 2.** (a) Uniform hazard spectra and (b) S_a hazard curves corresponding to the hazard
563 surface of Fig. 1.

564 **Fig. 3.** The effect of alternative structural modeling choices on the capacity curve of a 5-story
565 reinforced concrete building, as estimated via first-mode static pushover (adapted from Zeris
566 et al. 2007).

567 **Fig. 4.** Steel beam plastic hinge uncertainties and their effect: (a) cumulative distribution
568 functions of θ_{pc} , or the difference between hinge rotation at maximum moment and at
569 complete loss of strength (adapted from Lignos and Krawinkler 2011) and (b) the estimated
570 dispersion of the median response in spectral acceleration versus maximum interstory drift
571 terms for a 9-story frame (from Vamvatsikos and Fragiadakis 2010).

572 **Fig. 5.** IDA curves for a $T = 1$ s oscillator showing the distribution of the EDP response given
573 intensity s , and the estimation of the corresponding probability of exceeding a certain EDP
574 value of δ , $P[EDP > \delta | IM = s]$.

575 **Fig. 6.** Yield Point Spectra computed for the 1940 NS El Centro record. The response of a
576 system with yield displacement $\delta_y \approx 4$ cm, yield strength coefficient $C_y \approx 0.18$, and $T = 1$ s is
577 shown. The yield point falls on the $\mu = 2$ curve, indicating that the peak displacement is twice
578 the yield displacement (from Aschheim 2002).

579 **Fig. 7.** YFS contours at $C_y = 0.1, \dots, 1.0$ determined for an elastoplastic system ($\delta_y = 0.06$ m)
580 subjected to the hazard of Fig.1. The red “x” symbols represent three performance objectives
581 ($\mu = 1, 2, 4$ at 50%, 10% and 2% in 50yrs exceedance rates, respectively). The third objective

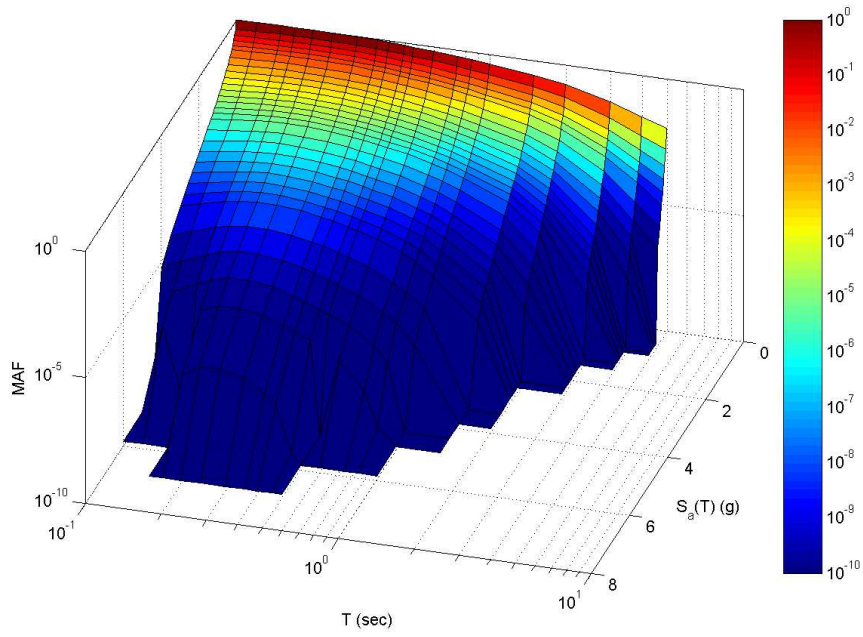
582 governs with $C_y \approx 0.93$. The corresponding period is $T \approx 0.51\text{s}$.

583 **Table 1.** Summary of different characteristics of design approaches.

Characteristic	Low fidelity	High fidelity
decision variable	structural response (DV=EDP)	cost, casualties, downtime, (actual DVs)
uncertainty propagation	None, probability controlled via input intensity only	Accurate, probability checked at output
design invariant term	Period or yield displacement via SDOF proxy	None, full MDOF is used

584

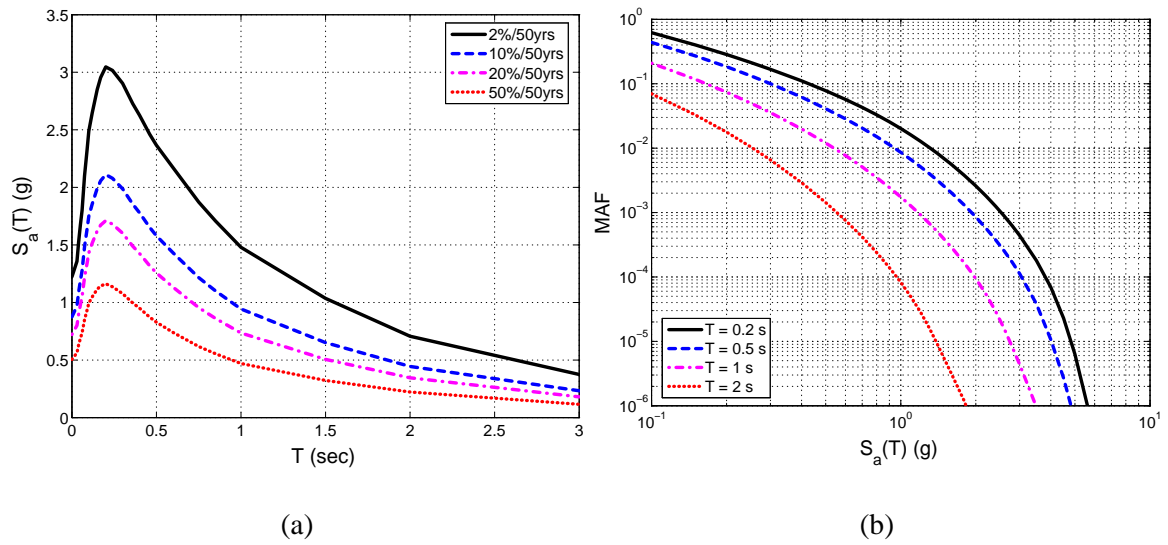
585



586

587 **Fig. 1.** Spectral acceleration hazard surface.

588

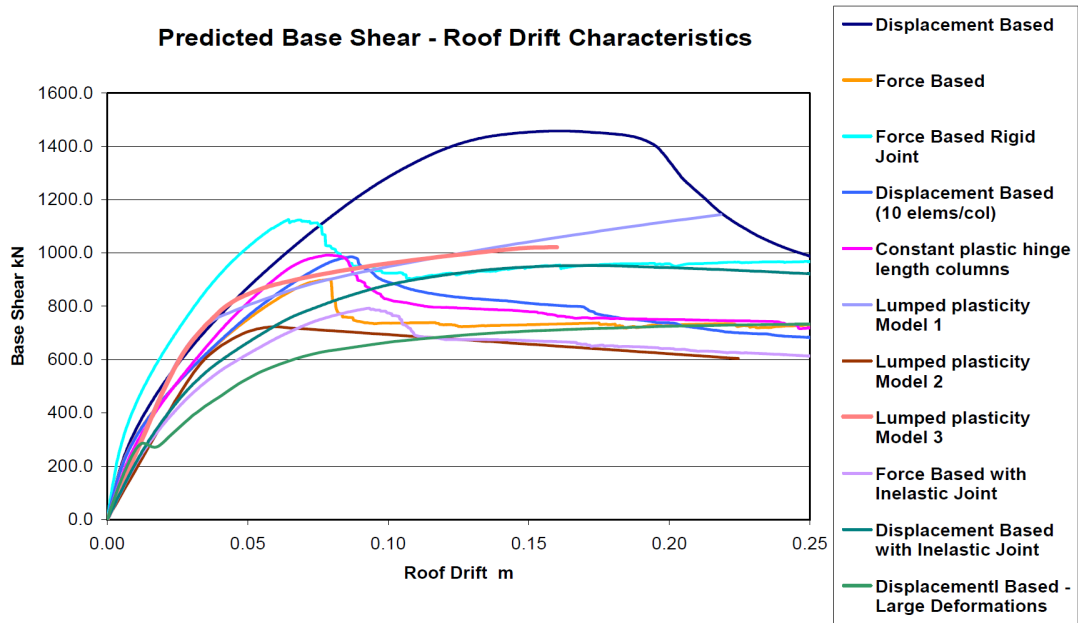


589 **Fig. 2.** (a) Uniform hazard spectra and (b) S_a hazard curves corresponding to the hazard surface of

590

Fig. 1.

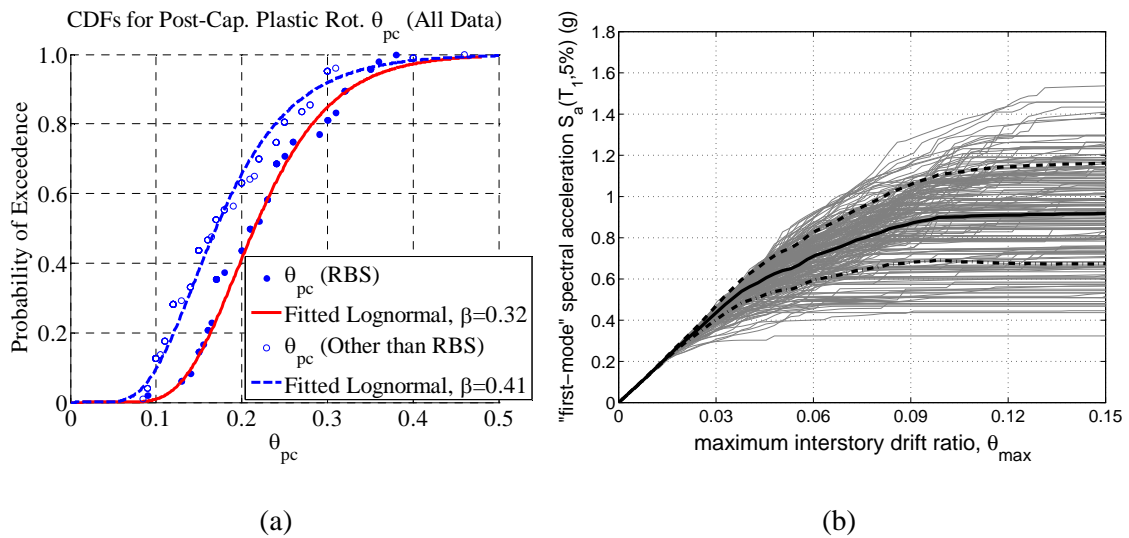
591



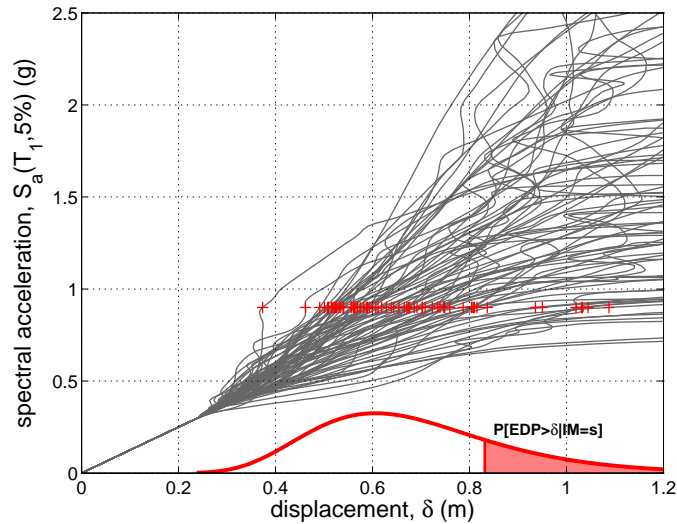
593

594 **Fig. 3.** The effect of alternative structural modeling choices on the capacity curve of a 5-story
 595 reinforced concrete building, as estimated via first-mode static pushover (adapted from Zeris et al.
 596 2007).

597



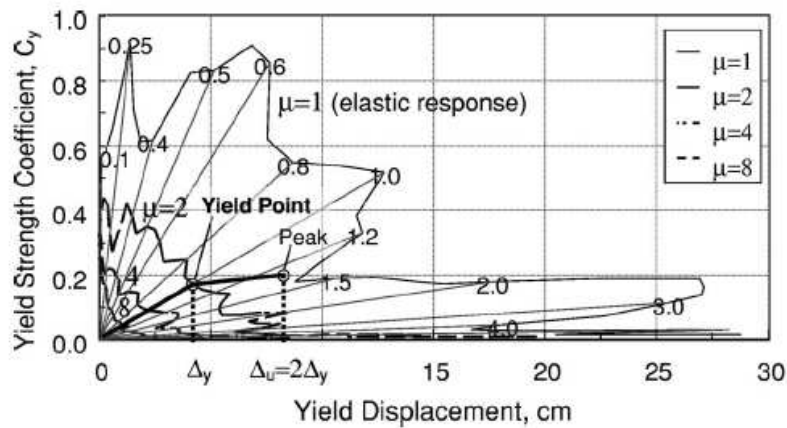
598 **Fig. 4.** Steel beam plastic hinge uncertainties and their effect: (a) cumulative distribution functions of
 599 θ_{pc} , or the difference between hinge rotation at maximum moment and at complete loss of strength
 600 (adapted from Lignos and Krawinkler 2011) and (b) the estimated dispersion of the *median* response
 601 in spectral acceleration versus maximum interstory drift terms for a 9-story frame (from Vamvatsikos



603

604 **Fig. 5.** IDA curves for a $T = 1$ s oscillator showing the distribution of the EDP response given intensity
 605 s , and the estimation of the corresponding probability of exceeding a certain EDP value of δ ,
 606 $P[EDP > \delta | IM = s]$.

607

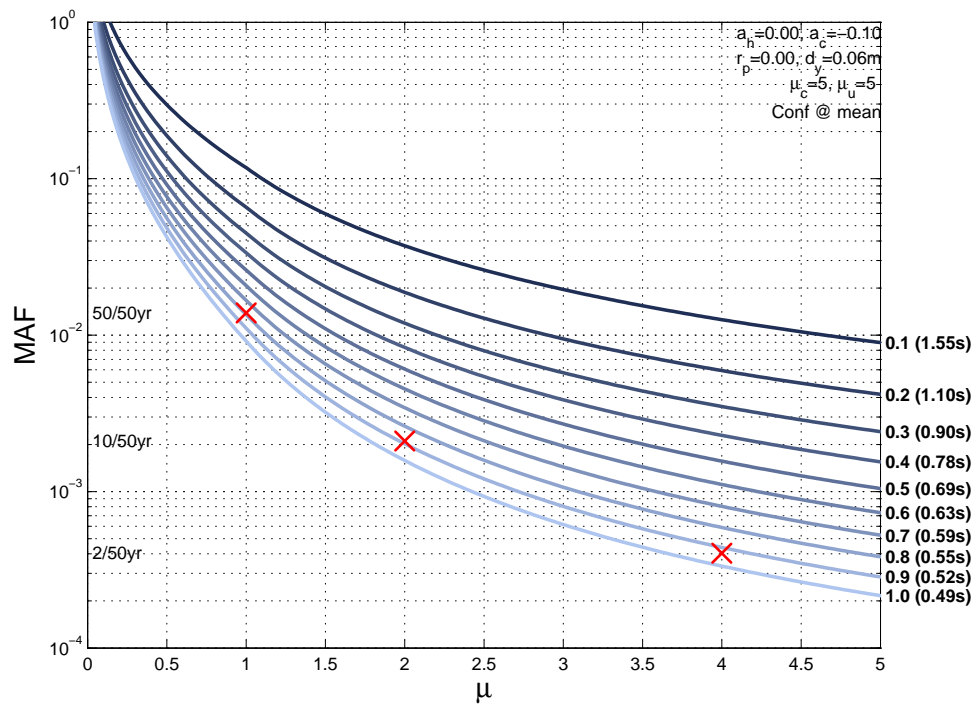


608

609 **Fig. 6.** Yield Point Spectra computed for the 1940 NS El Centro record. The response of a system
 610 with yield displacement $\delta_y \approx 4$ cm, yield strength coefficient $C_y \approx 0.18$, and $T = 1$ s is shown. The
 611 yield point falls on the $\mu = 2$ curve, indicating that the peak displacement is twice the yield
 612 displacement (from Aschheim 2002).

613

614



616

617 **Fig. 7.** YFS contours at $C_y = 0.1, \dots, 1.0$ determined for an elastoplastic system ($\delta_y = 0.06m$) subjected
 618 to the hazard of Fig.1. The red “x” symbols represent three performance objectives ($\mu = 1, 2, 4$ at
 619 50%, 10% and 2% in 50yrs exceedance rates, respectively). The third objective governs with $C_y \approx$
 620 0.93. The corresponding period is $T \approx 0.51s$.

621

622